NUKLEONIKA 2004;49(1):7–14

ORIGINAL PAPER

Experimental and theoretical investigations of crater formation in an aluminium target in a PALS experiment

**Stefan Borodziuk,
Igor Ya. Doskach,
Sergei Gus'kov,
Karel Jungwirth,
Milan Kálal,
Andrzej Kasperczuk,
Bozena Kralikova,
Edward Krousky,
Jiří Limpouch,
Karel Masek,
Miroslav Pfeifer,
Pawel Pisarczyk,
Tadeusz Pisarczyk,
Karel Rohlena,
Vladislav Rozanov,
Jiří Skala,
Jiří Ullschmied**

Abstract Experimental and theoretical results of investigations of the iodine laser – Al solid target interactions on the PALS (Prague Asterix Laser System) facility are presented. The experimental investigations of laser interaction with massive Al targets devoted to shock wave propagation in solids and crater formation physics are presented. Experiments were performed with the use of high intensity laser pulses ($10^{13–15}$ W/cm^2) for two laser wavelengths (0.438 μm and 1.315 μm) and four laser beam radii (from 35 μm up to 600 μm). The crater dimensions were measured using optical microscopy and a wax-replica technique. Plasma expansion out of the target was measured via three-frame interferometry. Theoretical model of the post-pulse crater formation by the shock wave propagating and decaying in solids after the end of the laser pulse is presented and applied for the explanation of the results obtained in experiments.

Key words laser-produced plasma • crater • absorption of laser radiation • resonance mechanism • inverse bremsstrahlung • interferometry • fast electrons

S. Borodziuk, A. Kasperczuk, T. Pisarczyk✉
Institute of Plasma Physics and Laser Microfusion,
23 Hery Str., 00-908 Warsaw, Poland,
Tel.: +48 22/ 683 70 96, Fax: +48 22/ 666 83 72,
e-mail: pisaro@ifpilm.waw.pl

I. Ya. Doskach, S. Gus'kov, V. Rozanov
P. N. Lebedev Physical Institute of RAS,
53 Leninski Ave., 119991 Moscow, Russia

K. Jungwirth, B. Kralikova, E. Krousky, K. Masek,
M. Pfeifer, K. Rohlena, J. Skala
Institute of Physics of the AS CR,
2 Na Slovance Str., 182 21 Prague 8, Czech Republic

M. Kálal, J. Limpouch
Faculty of Nuclear Sciences and Physical Engineering,
Czech Technical University in Prague,
7 Brehova Str., 115 19 Prague 1, Czech Republic

P. Pisarczyk
Institute of Computer Science,
Warsaw University of Technology,
15/19 Nowowiejska Str., 00-665 Warsaw, Poland

J. Ullschmied
Institute of Plasma Physics of the AS CR,
3 Za Slovankou Str., 182 21 Prague 8, Czech Republic

Received: 6 October 2003, Accepted: 10 December 2003

Introduction

Intense laser radiation incident on a solid target creates a hot and dense plasma. Apart from the direct plasma production as a result of laser beam – target interaction, the second important mechanism of the plasma creation is generation and propagation of the shock wave inside irradiated material. This is the reason of the crater creation.

Investigations of crater parameters, such as the shape and dimensions, deliver many interesting informations about the mechanisms of laser energy transfer into the target. It may be also regarded as a laser version of the so-called high velocity impact (HVI) problem [2]. The classical HVI problem occurs, when a real material macroparticle (projectile) strikes a solid target. In the laser version of HVI, we have the "virtual" projectile (i.e. the laser pulse) striking the target and producing a crater.

In this paper, we describe an experiment, which utilizes planar massive Al targets to study the crater formation process. The laser-produced crater investigation has a long history. A rewiev of the earlier stage of such investigations is presented in Ref. [1]. These experiments have been devoted to study the mechanisms of crater formation including matter evaporation and shock wave generation under the action of laser pulse with the intensity 10^8–10^{12} W/cm^2. Now, the problem is under active studying of both the laser matter interaction physics and laser processing at the level of laser pulse intensity of 10^{10}–10^{14} W/cm^2. One of the significant fields is the investigation of equation of state of metals on the basis of laser-produced crater experi-

ments [8]. In the field of laser processing, investigations of mechanical characteristics, conditions of splits, cracks and spallations are very important [5–7]. Aluminium, a very important technological material, is actively investigated as a target.

Our experiments are distinguished due to a wide range of values of laser energies, intensities and focal spot radii. We used two laser wavelengths (the first and third harmonics of an iodine laser). In particular, the range of parameters $I\lambda^2$ in our experiments is 10^{12}–10^{16} W/cm^2. An upper part of this range includes the conditions of resonant mechanism of laser light absorption and initiation of plasma instabilities and self-focusing process (see, for example, [3, 11, 12]). This allowed to investigate and compare the physics of laser-produced crater formation in both the mechanisms of laser pulse absorption: inverse bremsstrahlung and resonant, and to find the effects of fast electrons on energy transfer, shock wave generation and crater formation.

A three-frame interferometric system with automated image processing was used to study the plasma expansion.

In a theoretical approach, the results were interpreted using a simplified model of the laser target interaction. Inverse bremsstrahlung and resonant absorptions of the laser radiation were included, as well as the emission of fast electrons. The target ablation and shock wave propagation were also taken into account.

Comparison of the results obtained in experiments with those derived from the theory allows to draw conclusions regarding laser light absorption efficiency, efficiency of ablation loading (fraction of the absorbed laser energy transformed into the energy of the shock wave in a solid) and parameters of the plasma torch.

It is also important that some quantitative results were obtained using rather simple experimental and theoretical methods connected with the crater produced in the target instead of more complicated diagnostic techniques like ion emission and X-ray generation studies or application of advanced numerical codes.

Experimental set-up and measurement results

The experiment was carried out with the use of the PALS facility [14]. The plasma was generated by an iodine laser beam on the surface of a planar solid target made of aluminium, by means of an aspherical lens. Two harmonics of laser radiation, the first one with a wavelength of λ_1 = 1.315 μm and the third one with λ_3 = 0.438 μm, were used. The focal lengths of the lens were 627 mm for λ_1 and 600 mm for λ_3. For both wavelengths the laser heating beam was directed perpendicularly to the target surface. The investigation was carried out with laser energy $E_L \cong 100$ J, and pulse duration of 0.4 ns. Vacuum in the experimental chamber was at a level of 5×10^{-6} Torr.

A three-frame interferometric system with automated image processing was used to study the plasma expansion. A scheme of the three-channel interferometric diagnostics is presented in Fig. 1. The diagnostic system was illuminated by the third harmonic of the iodine laser. The delay between the frames was 3 ns, so that the interferometric measurement during a single shot covered a period of 6 ns only. In order to probe later stages of the plasma expansion, the period of observation in some shots was delayed by 6 ns. Due to the high reproducibility of the plasma expansion at different laser shots, interferogram sequences from different shots could be sewed together. Thanks to that, our observation period was extended up to 12 ns, starting from 3 ns after the maximum of the heating laser pulse. This initial moment corresponded actually to the beginning of the crater formation process [15].

The investigations were carried out at different levels of intensity of the laser radiation on the target. This intensity was reached by changing the focal lens position. The maximum of the intensity occurring in the focal point corresponded to the minimum focal spot radius of 35 μm. The investigation was carried out for the following focal spot radii: R_L = 35, 100, 300, and 600 μm.

Interferometric results

Interferometric measurements allowed us to observe the process of the outflow of plasma from the crater. Electron density distributions were obtained by means of special numerical methods, presented in paper [16]. The essential information about it are presented in Figs. 2 and 3. Figure 2 illustrates the outflow of plasma from the crater for the two wavelengths used. The plasma stream borders are

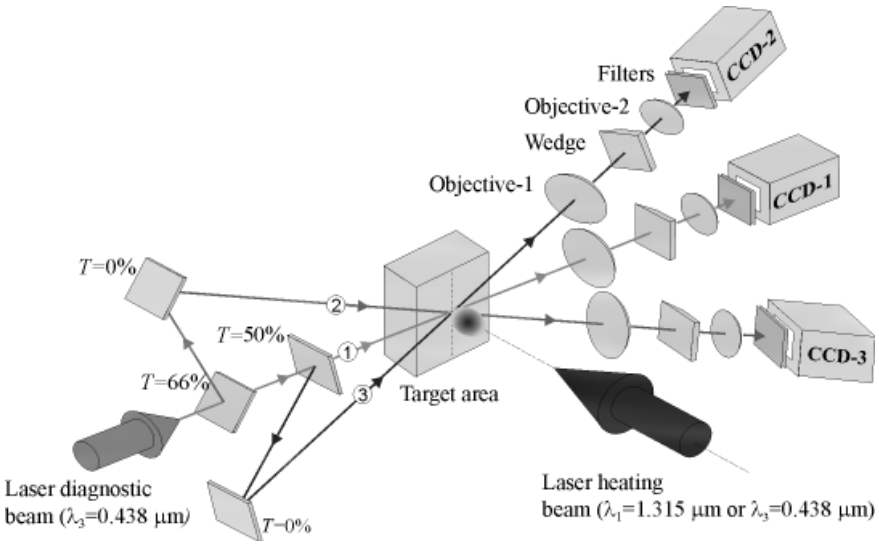

Fig. 1. Scheme of the three-channel interferometric diagnostics.

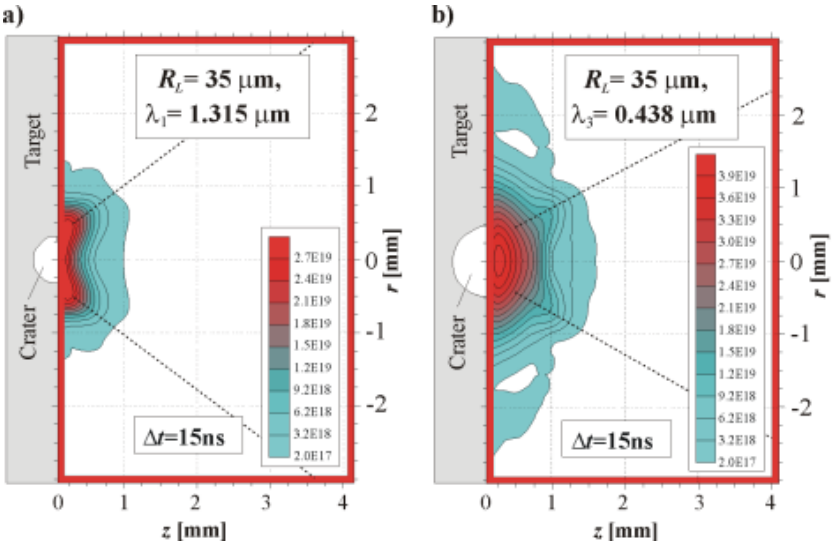

Fig. 2. Electron density in the plasma outflows from the craters for laser spot radius R_L = 35 μm and delay Δt = 15 ns at two different wavelengths: a) λ_1 = 1.315 μm; b) λ_3 = 0.438 μm. The oblique dotted lines denote an approximate boundary of the outflow from the crater.

represented here by the equidense of $n_e = 2 \times 10^{17}$ cm^{-3}. The second equidence corresponds to $n_e = 3 \times 10^{18}$ cm^{-3} and the next equidenses are distant to each other by $n_e = 3 \times 10^{18}$ cm^{-3}.

With the shorter wavelength, the plasma blob has dimensions approximately twice larger compared to the longer one. The more intensive outflow of plasma results in a bigger crater. The diagrams presented in Fig. 3 show the changes of total electron number as a function of time, for the same two cases. In the case of the longer wavelength, the outflow of plasma has approximately a uniform character (the total electron number is roughly conserved at a level of 2×10^{16}), while for the shorter wavelength the total electron number grows in time very fast, reaching a value of about 8×10^{16} at 15 ns. Thus, such diagrams can provide information on the dynamics of the crater creation process.

In other words, one may conclude that a shorter laser wavelength means a deeper laser penetration (higher critical density), and more efficient collisional absorption. Consequently, the laser-induced shock wave is stronger, so both the mass of the material ejected from the target and the crater volume are enhanced.

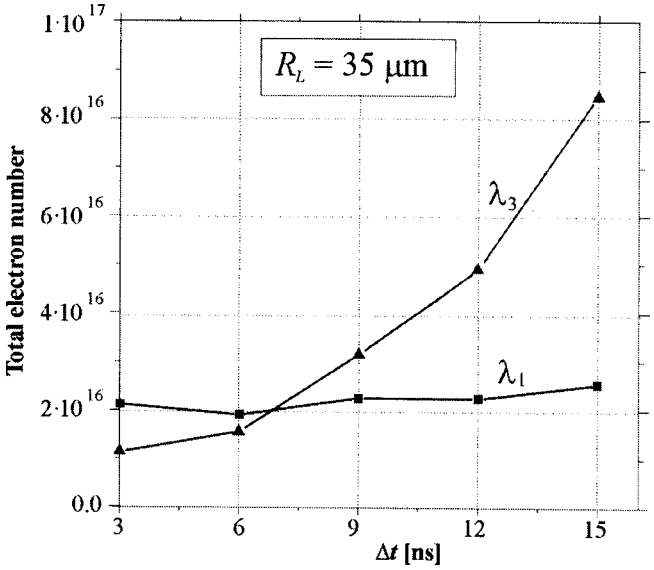

Fig. 3. Total electron number in the plasma outflow *vs.* time delay after laser.

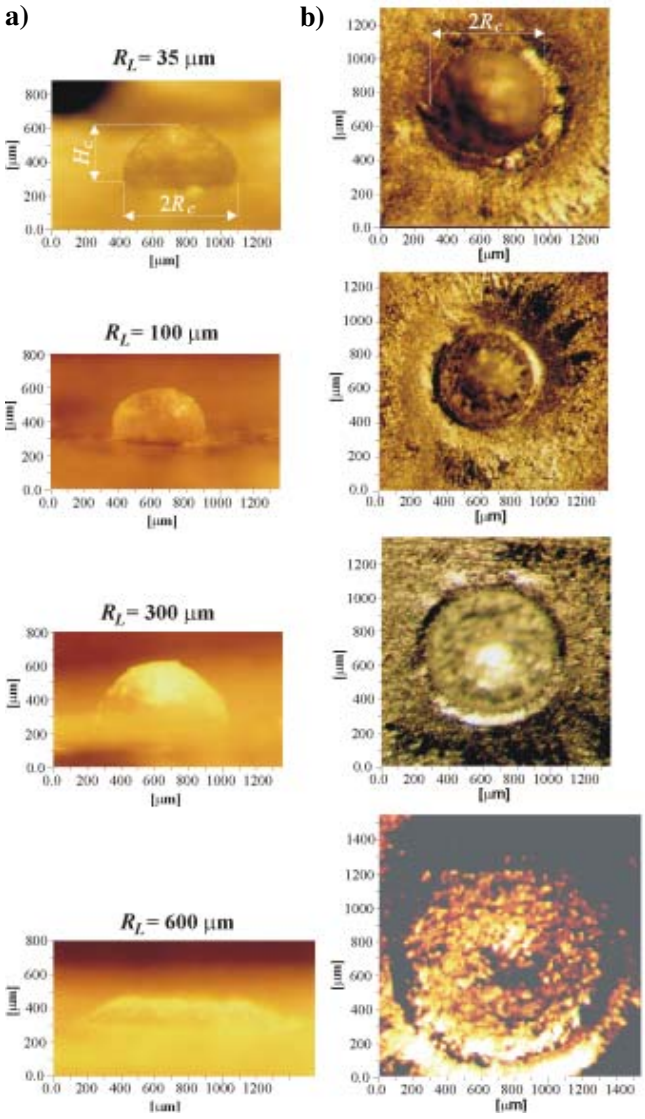

Fig. 4. Crater replicas photography obtained for the basic harmonic of heating laser beam (λ_1 = 1.315 μm) with energy of 100 J and different values of the focal spot radius: a) side view; b) top view.

Optical microscopy results

The crater dimensions were obtained by means of optical microscopy measurements. In order to obtain the shape of the craters, craters replicas were made of wax. The set of the actual replicas of the craters for the two harmonics of the laser radiation and different radii of the irradiation area are presented in Figs. 4 and 5. Most of the craters have regular shapes (hemisphere). For the same laser pulse energies (E_L = 100 J), the craters created in the experiment with a shorter laser wavelength (λ_3) are apparently larger, compared to those produced by λ_1 radiation.

Differences of the shapes and the dimensions of the craters for the analysed cases are clearly seen in Fig. 6.

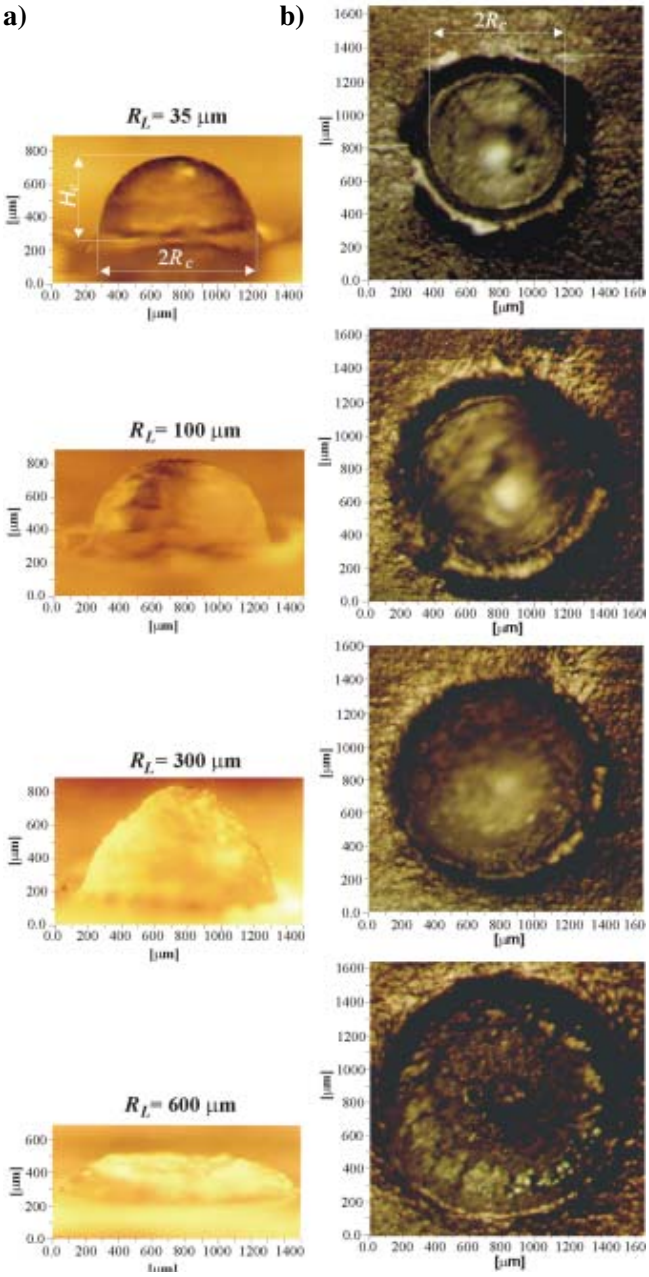

Fig. 5. Crater replicas photography obtained for the third harmonic of heating laser beam (λ_3 = 0.438 μm) with energy of 100 J and different values of the focal spot radius: a) side view; b) top view.

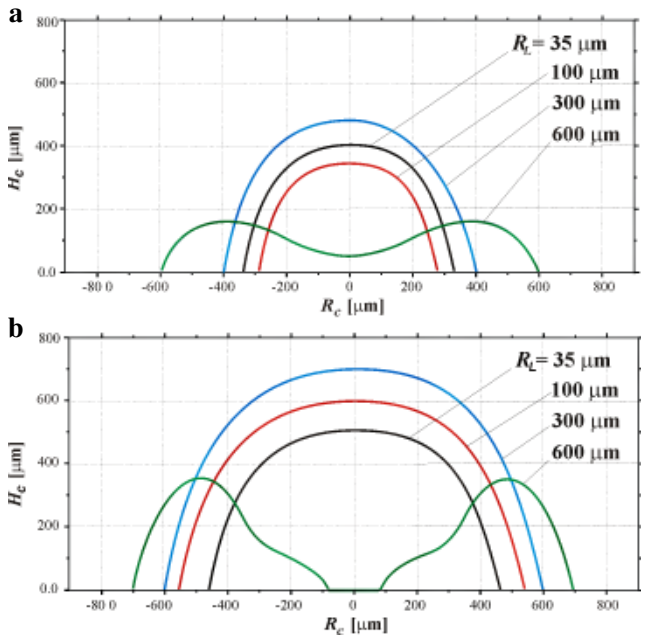

Fig. 6. Crater shapes and dimensions determined on the basis of wax crater replicas for basic (a) and the third (b) harmonics of heating laser beam.

While for the irradiation spot radii R_L = 35, 100, and 300 μm the difference only concerns the crater dimensions, in the case of R_L = 600 μm a completely different shape of the craters is observed.

Instead of the hemispherical form of the craters, a hemitoroidal character of the craters is observed. This effect is connected with some properties of the PALS iodine laser system. In comparison with a solid laser, the iodine, as a gas, laser has more nonuniform distribution of the energy on cross-section of laser beam. At the high intensity of laser radiation corresponding to small radii of the focused beam (R_L = 35 and 100 μm) such nonuniformities have not been effected on the form of the crater and the picture of interferometric measurements. This is explained by the fast processes of energy transfer in the evaporated part of the target at such high laser intensities and the formation, for this reason, enough smoothed distribution of the ablation pressure. The nonuniform ring of intensity distribution with a minimum intensity near the axis, peculiar to PALS laser, has been obviously displayed in both the interferometric picture of a plasma torch and the crater replica at the low intensities of the laser pulse corresponding to large radii of laser beam (R_L = 300 and 600 μm).

This situation concerns only the first harmonic of the laser radiation. In the case of the third harmonic, to have the laser energy E_L = 100 J, the output laser energy should be 2–3 times larger, mainly due to the wavelength transformation efficiency which is in the range of 30–50%. The concave character of the intensity distribution is even more pronounced in the case of the third harmonic due to the nonlinear transformation of the DKDP crystal.

In case of the small focal spot radii, the target irradiation constitutes approximately a point source and creates a hemispherical crater. When the focal spot radius becomes relatively large (e.g. 600 μm), intensity of the focused laser beam drops drastically and the shock wave generated under these conditions cannot reach the axis and is unable to transform to the hemispherical shape.

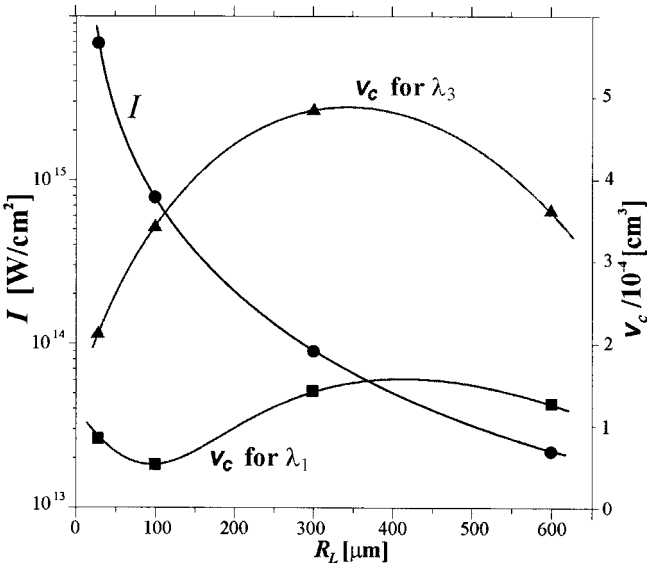

Fig. 7. Crater volumes *vs.* laser spot radius.

In Fig. 7, changes of the craters volume for the both wavelengths as a function of the focal spot radius (or laser irradiation intensity) are presented.

On the basis of Fig. 7, we could come to the following conclusions:

– The optimal value for the crater volume focal spot radius occurs to be about 300 μm. This value of R_L corresponds to $I \cong 10^{14}$ W/cm^2. It could be assumed that in these conditions absorption of the laser radiation is very effective, a lateral heat conduction should be rather small and there is no problem with fast electron generation. So, in these conditions a strong shock wave can be generated.
– The volume of the crater strongly depends on the wavelength of the laser radiation. An efficiency of the crater creation strongly grows with decreasing wavelength. This could be attributed to the higher losses of laser energy for the fast electron generation when the wavelength increases. So the transfer of the laser energy to the shock wave in this case is less effective.

Theoretical model

To interpret the experimental results we use a theoretical model [4] for modelling the laser radiation absorption and the crater creation. In this model, all the main physical processes taking part in the investigated phenomenon are included: laser energy absorption, matter evaporation and corona creation, energy transfer from the corona to the dense material of the target during the laser pulse, shock waves creation and propagation, matter melting by the shock waves and subsequent melted matter ejection from the growing crater.

In Table 1 the following values are presented:

– the experimental values: R_L – laser spot radius; E_L, I and λ, energy, intensity and wavelength of laser radiation, respectively; R_c and H_c – crater radius and depth, respectively; V_c – crater volume and M_c – crater mass;
– the theoretically calculated values: R_a – plasma torch

Table 1. The experimental and theoretically calculated values for modelling the laser radiation absorption and the crater creation.

		E_L = 100 J, λ_3 = 0.438 μm				E_L = 100 J, λ_1 = 1.315 μm			
Shot number		I_1^*	I_2	I_3	I_4	II_1^*	II_2^*	II_3	II_4
R_L	(μm)	35	100	300	600	35	100	300	600
I	(W/cm^2)	7.1×10^{15}	8.3×10^{14}	8.8×10^{13}	2.2×10^{13}	7.1×10^{15}	8.3×10^{14}	8.8×10^{13}	2.2×10^{13}
$I\lambda_2$	(W μm^2/cm^2)	1.3×10^{15}	1.5×10^{14}	1.7×10^{13}	4.2×10^{12}	1.2×10^{16}	1.4×10^{15}	1.5×10^{14}	3.8×10^{13}
					Experiment				
R_c	(μm)	475	550	600	700	330	280	400	630
H_c	(μm)	500	600	700	280	400	340	480	160
V_c	(cm^3)	2.1×10^{-4}	3.4×10^{-4}	4.9×10^{-4}	3.6×10^{-4}	8.8×10^{-5}	5.5×10^{-5}	1.4×10^{-4}	1.3×10^{-3}
M_c	(g)	5.7×10^{-4}	9.3×10^{-4}	1.3×10^{-3}	9.8×10^{-4}	2.4×10^{-4}	1.5×10^{-4}	3.9×10^{-4}	3.5×10^{-4}
					Theory				
R_a	(μm)	120	230	350	630	140	200	400	650
R_L/R_a		0.3	0.44	0.86	0.95	0.25	0.5	0.75	0.92
$\sigma = E_s/E_{ab}$		0.027	0.04	0.077	0.085	0.1	0.015	0.022	0.027
$D_\parallel$	(cm/s)	7.3×10^6	4.2×10^6	2.2×10^6	1.2×10^6	6.1×10^6	2.3×10^6	1.2×10^6	8.6×10^5
$D_\perp$	(cm/s)	6.6×10^6	3.2×10^6	10^6	4×10^5	4.5×10^6	1.2×10^6	3.1×10^5	1.7×10^5
τ_s	(ns)	6.8	14	32	24	6.6	15	32	18
$k_{ab} = E_{ab}/E_L$		0.34	0.37	0.27	0.19	0.039	0.16	0.28	0.21

* In these cases the resonant absorption mechanism is responsible for the significant part of energy absorption.
** This case corresponds to the resonant absorption mechanism dominance.

radius near the evaporation boundary; $\sigma = E_s/E_{ab}$ – efficiency of ablation loading, E_s – energy transformed to the shock wave propagating in the condensed part of the target, E_{ab} – absorbed laser energy; $D_\parallel$ and $D_\perp$ – shock wave velocities along the direction of laser beam axis and in the transverse direction, respectively; τ_s – duration of crater-creating shock wave propagation; $k_{ab} = E_{ab}/E_L$ – laser energy absorption coefficient.

First of all, the main general features of the conditions of laser-plasma interaction and the measured results should be noted. For the shots (I_1^* and II_1^*, II_2^*) when the values of parameter $I\lambda^2$ are greater than 10^{14} W μm^2/cm^2, the resonance mechanism gives a significant contribution to the laser radiation absorption together with inverse bremsstrahlung process and one must take into account that some fraction of the absorbed laser energy (20–30%) transforms into the energy of fast electrons. Other shots (I_2–I_4, II_3 and II_4) have been performed under conditions when the parameter $I\lambda^2$ was close to or less than the value 10^{14} W μm^2/cm^2 and it seems reasonable to assume that the laser light was absorbed as a result of the inverse bremsstrahlung process, without generation of fast electrons.

To describe the ablation pressure formation, we use a self-similar solution for the isothermal expanding of the given mass of matter [13].

Taking into account the two-dimensional effect we can get an expressions for the main parameters of laser-produced torch: ρ_a, c_a, p, which is the density, sound velocity and pressure of the plasma near the surface of evaporation, respectively.

Additionally, taking the advantage of [9], we can get expressions for the ablation pressure in the cases of bremsstrahlung and resonance absorption mechanisms, respectively:

$$(1)\quad P_{aB} \approx 1.6\cdot 10^3 \cdot \frac{k_{ab}^{2/3}\cdot I_L^{2/3}}{\lambda^{2/3}} \cdot \left(\frac{\mathrm{A}}{Z}\right)^{2/3} \cdot \left(\frac{R_L}{R_a}\right)^2, \quad \mathrm{erg/cm^3}$$

$$(2)\quad P_{aR} \approx 2.9\cdot 10^{-7} \cdot \frac{k_{ab}^{1/2}\cdot I_L^{2/3}\cdot \lambda}{\tau_L^{1/2}\left(2+Z\right)^{1/4}} \cdot \left(\frac{\mathrm{A}}{Z}\right)^{2/3} \cdot \left(\frac{R_L}{R_a}\right)^2, \ \mathrm{erg/cm^3}$$

where: k_{ab} – laser radiation absorption coefficient; I_L, λ and τ_L – intensity, wavelength and duration of laser pulse measured in W/cm^2, μm and second, respectively; $R_a = R_L + c_a\tau_L$ – radius of plasma torch which is the radius of laser beam enhanced for the distance of transverse thermal expanding of the matter; A and Z – atomic weight and ionisation degree.

The process of the laser pulse action on the target is characterized by the efficiency of ablation loading, which represents the fraction of absorbed laser energy E_{ab}, transferred into the shock wave energy E_s (see [10]):

$$(3)\quad \sigma = \frac{E_s}{E_{ab}} = \frac{2}{\gamma_s+1}\cdot\frac{D_s}{k_{ab}}\frac{P_a}{I_L} = \left[\frac{12}{\pi\left(\gamma_s+1\right)}\right]^{1/2}\left(\frac{\rho_a}{\rho_s}\right)^{1/2}.$$

In this expression, γ_s is the adiabatic exponent in the condensed matter, ρ_s is the density of condensed matter and D_s is the shock wave velocity. The shock wave velocity is given by

$$(4)\quad D_s = \left[\frac{2}{\gamma_s+1}\cdot\frac{p_a}{\rho_s}\right]^{1/2}.$$

Using eq. (1) and eq. (2) in eq. (3) we can get the efficiency of ablation loading for both the absorption mechanisms

$$(5)\quad \sigma_B = \left[\frac{12}{\pi\left(\gamma_s+1\right)}\right]^{1/2}\cdot\left[\frac{3}{\pi}\left(\frac{\gamma_a-1}{3\gamma_a-1}\right)\right]^{1/4}\cdot\left(\frac{\rho_{cr}}{\rho_s}\right)^{1/2} \cdot\frac{R_L}{R_a} \approx 2.7\cdot 10^{-2}\,\frac{\left(\frac{\mathrm{A}}{Z}\right)^{1/2}\cdot\left(\frac{R_L}{R_a}\right)}{\lambda\cdot\rho_s^{1/2}},$$

$$(6)\quad \sigma_R = 6.8\cdot 10^{-17}\,\frac{I_L^{1/2}\cdot\lambda^{3/2}\cdot\left(\frac{\mathrm{A}}{Z}\right)^{3/2}\cdot\frac{R_L}{R_a}}{k_{ab}^{1/4}\cdot\tau_L^{3/4}\cdot\left(2+Z\right)^{3/8}\cdot\rho_s^{1/2}}.$$

In the above expressions, γ_a (the adiabatic exponent of the plasma torch) = 5/3 as for ideal gas and $\gamma_s = 3$ was used [13] for our case of aluminium target. The ablation loading efficiency in the case of bremsstrahlung absorption is nearly proportional to λ^{-1} and in case of the resonance absorption its dependence on the pulse parameters is more complex. In particular, at the resonant absorption the ablation loading increases while the wavelength grows because of the fast electron energy strong increase as the wavelength grows.

Additionally, we need also to know the crater mass. It can be approximated by the mass of matter melted by the shock wave. According to [10], this mass can be calculated from the following simple formula:

$$(7)\quad M_c = \frac{\sigma\cdot k_{ab}\cdot E_L}{4\varepsilon}$$

where: $\varepsilon \approx 4\times 10^2$ J/g is the specific energy of melting of the aluminium in the atmospheric conditions.

In our experiments, the melting of the material and the crater formation occurred under a shock wave action when the pressure of 1 Mbar and more was realized in the region of interaction. In formula (7), it is assumed that the specific energy, which is needed to melt aluminium in these conditions, is the melting energy ε corresponding to the current atmospheric conditions but increased, approximately, by a factor of 4 [17]. The factor 4 takes into account the heating of the material up to the temperature of melting, distribution between thermal and elastic energies of the Al equation of state, distribution between thermal and kinetic energy in the shock wave [17].

Comparison of the crater mass measured in the experiment with that theoretically calculated allows us to get information about the amount of laser energy absorbed in the target or, in other words, the absorption coefficient k_{ab}.

The shock wave velocity can be evaluated from the efficiency of ablation loading using (3):

$$(8)\quad D_s = \left(\frac{\sigma\cdot k_{ab}\cdot I_L}{\rho_s}\right)^{1/3}.$$

So, the time of crater-creating shock wave can be estimated as

$$\tau_s = \frac{H_c}{D_s}. \quad (9)$$

Discussion

The experiments aimed at the crater creation by the action of the relatively short laser pulses of different wavelengths and intensities allow to study some important phenomena of the laser plasma torch evolution and shock wave propagation in solids.

Duration of laser pulse (τ_L = 0.4 ns) is much less than the time of crater-produced shock wave decay (several tens of nanoseconds). For this reason, the matter evaporation time by laser pulse is much less than the matter emission from the crater by the shock wave. The velocity of laser-evaporated matter v_h is much higher than that of the shock wave-emitted matter v_c: $v_h/v_c \approx (\rho_0/\rho_{cr})^{1/2}$ (here ρ_0 is the density of solid Al, ρ_{cr} is the critical density); $v_h \approx (3–7) \times 10^7$ cm/s; $v_c \approx (2–4) \times 10^6$ cm/s.

These features are illustrated by the data in Fig. 3. To calculate the emitted mass of matter on the basis of total number of plasma free electrons, a value of the average ion charge Z in the range 4–8 could be used. Such values of ion charge are obtained by the estimation in the Saha approximation [14] in the plasma temperature range of 100–200 eV, which is given by formulas (1) and (2) at the plasma density corresponding to the interferometric measurements – 10^{17}–10^{18} cm^{-3}. For example, the total numbers of electrons at the average ion charge $Z = 5$ correspond to the mass of the emitted matter of 7×10^{-7} g (λ_3 = 0.438 μm) and 2×10^{-7} g (λ_1 = 1.315 μm). These values are by three orders of magnitude smaller than the total extracted crater masses (5.7×10^{-4} g for λ_3 = 0.438 μm and 2.7×10^{-4} g for λ_1 = 1.315 μm) and mainly correspond to the masses of laser-evaporated matter. Nevertheless, the increase of total electron number after 6 ns for the third harmonic represents the contribution of shock wave-emitted mass. Beginning time of this contribution is the time during which the ions with the velocity $v_h \approx 4 \times 10^6$ cm/s fly the half of plasma torch length, approximately 500 μm. This time is about 10 ns, which is in good agreement with experimental data.

The dependencies of σ and k_{ab} (the ablation loading efficiency and the laser energy absorption coefficient) on the laser spot radius are shown in Fig. 8. Let us remind, both the values, σ and k_{ab}, were obtained by the solution of equation (7) in which the right part is given by the value of experimentally measured mass of crater and the value of the ablation loading efficiency σ was given by (5) or (6). Ablation loading efficiency σ depends on the absorption efficiency k_{ab}. So, firstly, the value of k_{ab} was defined from equation (7), and then this value was substituted in the formula (5) or (6) yielding the value of σ. One can see a dramatic fall of k_{ab} and a rise of σ for R_L = 35 μm at the laser wavelength λ_1 = 1.315 μm at bigger laser spot radii. This effect is due to the laser absorption mechanism change, for the first harmonic in particular.

For the bremsstrahlung absorption mechanism of the laser radiation, the efficiency of ablation loading increases at the decreasing laser radiation wavelength. For the planar laser plasma expansion the efficiency of ablation loading does not depend on the laser pulse intensity and increases linearly at the decreasing laser radiation wavelength. Two-dimensional effects of the laser-produced plasma torch expansion sufficiently decrease the efficiency of ablation loading at the decreasing laser spot radius. The decrease of the absorption coefficient for the smaller radii is caused by the transition from the bremsstrahlung absorption to the resonant one. For the shorter wavelength (the third harmonic) this transition occurs at higher laser intensities (at smaller focal spot radii).

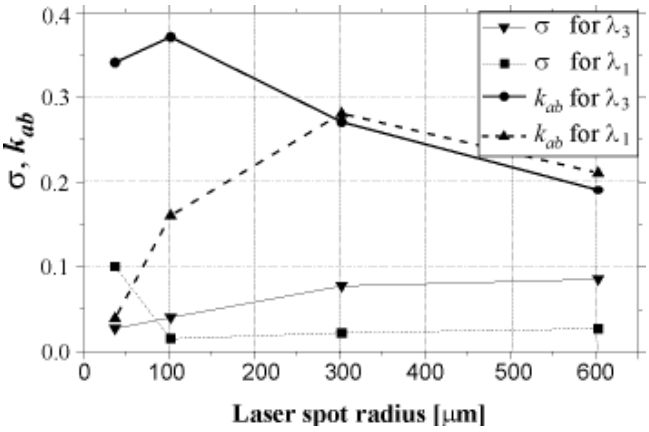

Fig. 8. Laser energy absorption coefficient and the ablation loading efficiency for different shots.

In Fig. 9, the ratio of the energy transferred into the shock wave to the laser pulse energy is presented. This coefficient $\eta = \sigma k_{ab}$ shows the overall efficiency of energy transfer at the crater creation and corresponds to the mass of the ejected matter. It is obvious that η is substantially larger for the shorter wavelength. For the first harmonic, a strong absorption coefficient decrease for small R_L is compensated for by a sharp increase of the ablation loading. When the laser intensity increases and the wavelength decreases, the average value of shock wave longitudinal velocity (along the laser pulse propagation direction) increases as $I^{1/2} \lambda^{-1/3}$. This velocity in the considered conditions falls within the range of $(1–5) \times 10^6$ cm/s. The transversal velocity of the shock wave near the crater hole is 1.5–2.5 times lower than the longitudinal one. The duration of decay of the crater-creating shock wave is at an interval of 7–30 ns for different shots.

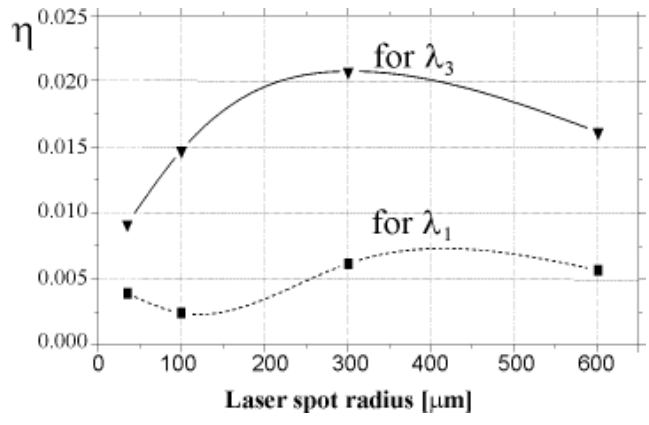

Fig. 9. Total laser energy transfer to the shock wave coefficient η.

Concluding remarks

We studied (experimentally and theoretically) the problem of crater formation on the surface of a solid Al target irradiated by intense light of the iodine laser beam. It may be regarded as a laser version of the so-called high velocity impact (HVI) problem.

Our main interest to study the crater formation was as follows: there were a number of experiments of laser produced plasma when many different diagnostic and theoretical methods were applied to study plasma properties but much less work was done to deal with the crater formation and to deduce plasma properties in such experiments. The important purpose of our work was to analyse some physical effects in plasma, applying the simple theoretical method which takes advantage of craters produced in targets irradiated by lasers.

One of the obvious advantages of such treatment is that we are able to measure the fundamental parameters describing the crater produced in our experiment (i.e. the crater dimensions R_c, H_c and the crater volume V_c or mass M_c) and this can be done very precisely in any time after the experiment was made.

In our further investigations of craters, we intend to use targets made from other materials and to apply a different laser method of projectile acceleration (using the double target technique).

Acknowledgments The work was partially supported by the European Committee programme Transnational Access to Research Infrastructures under contract HPRI-CT-1999-0053 (PALS project 013), the Russian Foundation of Basic Research (Project # 02-02-16966) and by INTAS under the contract INTAS-01-572. Additional support was also provided by the International Atomic Energy Agency under the IFE-CRP, CZR-11655. All these financial supports are gratefully acknowledged.

References

1. Anisimov SI, Imas YaI, Romanov GS, Khodiko YuV (1970) The hydrodynamic regime of destruction. In: Bonch-Bruevich AM, El'yashevich MA (eds) The interaction of high-power radiation with metals. Nauka, Moscow, pp 178–217
2. Borodziuk S, Kasperczuk A, Pisarczyk T *et al.* (2003) Application of laser simulation method for the analysis of crater formation experiment on PALS laser. Czech J Phys 53:799–810
3. Bychenkov VYu, Tikhonchuk VT (1993) Laser-target interaction: laser energy absorption and nonlinear plasma phenomena. In: Velarde G, Ronen Y, Martinez-Val JM (eds) Nuclear fusion by inertial confinement. CRC Press, Inc., Boca Raton, Florida, pp 73–94
4. Doskach IYa, Pisarczyk T, Gus'kov SYu *et al.* (2003) Laser-produced post-pulse crater formation in solids observed in PALS facility interaction experiment. Proc of SPIE 5228:121–130
5. Eliezer S, Gazit Y, Gilath I (1990) Shock wave decay and spall strength in laser-matter interaction. Appl Phys 68:356–358
6. Eliezer S, Gilath I, Bar-Noy T (1990) Laser-induced spall in metals: experiment and simulation. J Appl Phys 67:715–724
7. Eliezer S, Moshe E, Ludmirsky A *et al.* (1997) A critical phenomenon for the spall strength in aluminum at strain rates larger than 10^7 s^{-1}. In: Miley GH, Campbell EM (eds) Proc of the 13th Int Conf on Laser Interactions and Related Plasma Phenomena, 15 April, Monterey, Woodbury, USA. AIP, vol. N 406, pp 653–660
8. Fortov VE, Kostin VV, Eliezer S (1991) Spallation of metals under laser irradiation. J Appl Phys 70:4531–4542
9. Gus'kov KS, Gus'kov SYu (2001) Efficiency of ablation loading and the limiting destruction depth of material irradiated by a high-power laser pulse. Quantum Electron 31:305–310
10. Gus'kov SYu, Zverev VV, Rozanov VB (1983) Steady-state model of the corona of spherical targets allowing for energy transfer by fast electrons. Quantum Electron 13:498–502
11. Hauser T, Scheid W, Hora H (1992) Theory of ions emitted from a plasma by relativistic self-focusing of laser beams. Phys Rev A 45:1278–1281
12. Hora H (2000) Ponderomotive and relativistic self-focusing. In: Laser plasma physics: forces and the nonlinearity principle. SPIE Press Monograph, vol. PM75, pp 104–112
13. Imshennik VS (1960) Isothermal expantion of finite mass of gas. Dokl Akad Nauk 5:263–267
14. Jungwirth K, Cejnarova A, Juha L *et al.* (2001) The Prague Asterix Laser System PALS. Phys Plasmas 8:2495–2501
15. Kasperczuk A, Pisarczyk P, Pisarczyk T *et al.* (2001) Interferometric investigation of an early stage of plasma expansion with the high-power laser system PALS. Czech J Phys 51:395–404
16. Kasperczuk A, Pisarczyk T (2001) Application of automated interferometric system for investigation of the behaviour of a laser-produced plasma in strong external magnetic field. Opt Appl 31:571–597
17. Zel'dovich YaB, Raizer YuP (1967) Physics of shock waves and high-temperature hydrodynamic phenomena. In: Hayes WD, Probstein RF (eds) Hypersonic flow theory, 2nd ed. Academic Press, New York–London, vol. 1, pp 685–710